

## The radio structure of 3C 309.1 determined by multi-baseline interferometry

A. J. Kus<sup>★</sup>, P. N. Wilkinson and R. S. Booth

*The University of Manchester, Nuffield Radio Astronomy Laboratories, Jodrell Bank, Macclesfield, Cheshire SK11 9DL*

Received 1980 June 23

**Summary.** We present hybrid maps of the radio structure of the QSO 3C 309.1 at 1666 MHz from observations with the European VLBI network and with radio-linked interferometers at Jodrell Bank. Our maps reveal that 3C 309.1 has a triple structure with a dominant compact self-absorbed core, extended in  $pa\ 162^\circ \pm 2^\circ$ , and symmetrically disposed on either side of this are two relatively extended outer lobes defining an overall  $pa$  of  $\sim 90^\circ$ . This dramatic change in position angle from milliarcsec to the arcsec scale is also seen in many of the asymmetric, core-dominated (D2) quasars, and thus 3C 309.1 appears to be intermediate in its properties between the symmetric (D1) and the D2 classes. It may in fact be a D1 quasar observed nearly end-on, with a relativistically enhanced nuclear core.

### 1 Introduction

The powerful radio source 3C 309.1 has a straight, steep ( $\alpha = -0.69$ ;  $S \propto \nu^\alpha$ ) spectrum between 1 and 10 GHz, and an overall extent of  $\leq 2$  arcsec (Wilkinson 1972); it is identified with a relatively bright QSO ( $V = 16.78$  mag,  $z = 0.904$ ) (Burbidge & Burbidge 1969). This combination of radio properties is unusual for a source of high intrinsic luminosity. Normally such luminous steep-spectrum sources are D1 ‘classical doubles’ whose maximum extent is  $> 100$  kpc, whereas asymmetric core-dominated (D2) sources with linear sizes similar to 3C 309.1 (i.e.  $< 100$  kpc) have very different spectra – often with a high-frequency excess (e.g. Readhead *et al.* 1978). Until recently it has not been possible to make detailed maps of such a compact source as 3C 309.1 and consequently our knowledge of its radio structure was sketchy. At 408 and 1423 MHz Wilkinson (1972) showed that the source is extended by  $\sim 1.3$  arcsec (FWHM) in  $pa \sim 85^\circ$ , while at 5 GHz Ryle & Elsmore (1973) found that their data were consistent with two equal components separated by 0.75 arcsec in  $pa \sim 75^\circ$ . Early VLBI observations indicated that the source possesses at least two components each  $< 0.03$  arcsec in diameter (Clark *et al.* 1968; Kellermann *et al.* 1971) with a separation  $0.030$  arcsec in  $pa\ 162^\circ.5 \pm 1^\circ.5$  (Fort 1971).

<sup>★</sup> On leave from Nicolaus Copernicus University, Institute of Astronomy, Torun, Poland.

In this paper we report the results of recent 18-cm observations of 3C 309.1 with four telescopes in the European VLBI network. Combining these observations with existing Jodrell Bank radio-linked interferometer data, we derive hybrid maps of the brightness distribution (from the fringe amplitudes only) with resolutions of 30 milliarcsec and 0.3 arcsec. Our results are in general agreement with the previous work, but the hybrid maps show that the overall source structure is triple and they highlight the dramatic change in the position angle from the milliarcsec to the arcsec structure. The study presented here is a part of a larger programme for investigating the details of the angular structures of several of these unusual radio sources, which are compact and yet have steep spectra.

## 2 The observations

The VLBI observations were made on 1978 January 7 and 9 at a frequency of 1666 MHz using four European network stations at Dwingeloo, Effelsberg, Jodrell Bank and Onsala; circularly polarized feeds were used on each telescope. The parameters of the telescopes and receiving systems are given in Table 1. Data were recorded on video tapes using the standard NRAO Mark II VLBI system (Clark 1973) with a bandwidth of 2 MHz. Rubidium frequency-standards were used at Jodrell Bank and Dwingeloo, while Effelsberg and Onsala were equipped with hydrogen masers. The video tapes were cross-correlated using the three-station VLBI processor at the Max-Planck-Institut für Radioastronomie (MPIfR) Bonn.

The correlated flux density on the VLBI baselines was calibrated by observing BL Lac and OQ 208, which were assumed to be unresolved on all baselines. Zero-baseline flux densities of both calibrators were measured at 1666 MHz by J. R. Baker using the 100-m telescope at Effelsberg shortly after the VLBI session. A summary is given in Table 2. Most of the individual fringe-amplitude points have  $\sim 5$  per cent errors dominated by calibration uncertainties, although correlator errors lead to uncertainties of  $\sim 10$  per cent in some points.

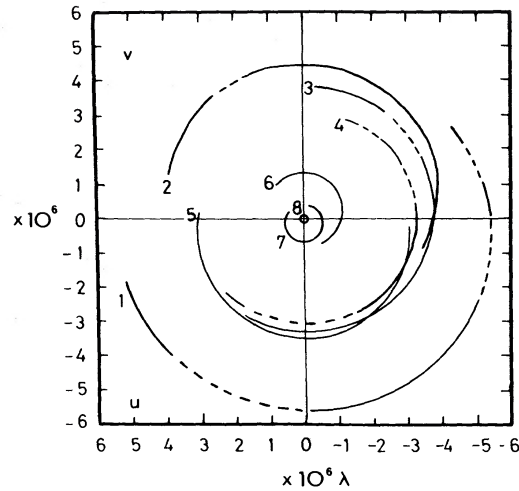
In addition to the VLBI data, we used existing observations from Jodrell Bank radio-linked interferometers to assist with the investigation of the extended structure. Measurements made with the Mk II—Defford interferometer at a wavelength of 18 cm were kindly supplied by A. Tzanetakis, and we also used 1423-MHz Mk I—Mk III measurements (Wilkinson 1973). The fringe visibilities at 1423 MHz were further averaged to produce points at 1-hr intervals and then multiplied by the zero-baseline flux density of 3C 309.1 at 1666 MHz.

Table 1

Location	Diameter (m)	System noise temperature (K)	Sensitivity (K/Jy)
Dwingeloo	25	42	0.11
Effelsberg	100	62	1.6
Jodrell Bank	76	120	0.82
Onsala	26	30	0.10

Table 2. Total flux densities at 1666 MHz measured in 1978 January.

Source	Total flux density (Jy)
3C 309.1	$7.02 \pm 0.03$
BL Lac	$3.51 \pm 0.03$
OQ 208	$1.00 \pm 0.01$



**Figure 1.** The  $u$ - $v$  coverage for 3C 309.1. The solid lines represent the regions covered by the observations. The VLBI baselines are 1. Jodrell Bank–Onsala, 2. Effelsberg–Onsala, 3. Effelsberg–Jodrell Bank, 4. Onsala–Dwingeloo, 5. Dwingeloo–Jodrell Bank, 6. Effelsberg–Dwingeloo. The Jodrell Bank baselines are: 7. Mk II–Defford, 8. Mk I–Mk III.

This assumes that the source components have similar spectral indices between 1423 and 1665 MHz.

The  $u, v$  loci of all these interferometers are presented in Fig. 1. The VLBI baseline lengths are between  $0.85$  and  $5.6 M\lambda$ , while the Jodrell Bank baselines range from  $0.1$  to  $0.65 M\lambda$ .

### 3 The brightness distribution

#### 3.1 ANALYSIS TECHNIQUES

Since this was the first experiment to be processed on the MPIfR processor, we were not surprised to encounter some problems with the closure phase data and eventually decided not to rely on it. Thus we were unable to apply the standard ‘hybrid-mapping’ procedure (Readhead & Wilkinson 1978) and so we determined the source brightness distribution from the fringe amplitudes only, using a method similar to the one proposed by Fort & Yee (1976) and extended by M. H. Cohen (see Wilkinson *et al.* 1977). An initial model of the source was Fourier transformed to give a visibility phase at each  $u, v$  point and these phases, taken together with the observed visibility amplitudes, were Fourier inverted to make a map. Then the CLEAN technique (Högbom 1974) was used to reduce the sidelobe level on this map. From the CLEAN map, new phases were calculated and from these, together with the observed amplitudes, a second CLEAN map was determined and so on. At each stage, the delta functions which comprised the map were used to calculate fringe amplitudes which were then compared with the observed data. The convergence of the procedure was checked both by visual inspection of the changes in the brightness distribution on successive maps and from the fit to the observed amplitudes. In order to speed up convergence, a good initial model is required and so some care was taken to obtain fairly good fits to the data on all baselines by means of a model-fitting program. The method outlined above then converges to a stable solution for the reasons described by Readhead & Wilkinson (1978). Since no phase information was used in these reconstructions we shall continue to refer to them as ‘hybrid’ maps following Baldwin & Warner (1978).

This procedure was used to make two sets of hybrid maps:

- (i) a  $2.2 \times 2.2$  arcsec map made from all the data with the full resolution of 30 milliarcsec,

(ii) a map made from the three shortest baselines only, with 0.3 arcsec resolution, covering  $3.2 \times 3.2$  arcsec.

We did this because of the limit to our computer array size ( $128 \times 128$ ). As contributions from all parts of the source can be seen on all baselines, we made a full-resolution map from all the data over as large an area as we could ( $2.2 \times 2.2$  arcsec), so that the reconstruction of the central component would not be distorted by the omission of significant components in the CLEAN process. Since our array-space limitation made it impossible to convolve this map with a larger beam to bring out reliably the details of the low-brightness extended structure, to make a bigger map we used data from the three shortest baselines only and restored with a 0.3-arcsec beam.

### 3.2 THE STRUCTURE OF THE CENTRAL COMPONENT

The final hybrid map (Fig. 2) of the compact component was obtained after four iterations using the data on all baselines. This map is merely the central portion ( $0.5 \times 0.5$  arcsec) of the full-resolution map just described. The present data are not sufficient to reconstruct its structure in other than broad outline and there is the unavoidable  $180^\circ$  ambiguity because this is a phaseless map, but it is clear that the basic position angle is  $162^\circ \pm 2^\circ$ , in agreement with Fort (1971). In cases like this, where components are comparable to the size of the restoring beam, model-fitting can be complementary to mapping and can provide at least some indication of the structure on scales smaller than the beam. Our two best models consisted of three and four collinear components with an overall extent of  $\sim 40$  milliarcsec and an overall width  $\leq 6$  milliarcsec. In both cases, at least one of the outer components points towards the extended ( $\sim 1$  arcsec) structure (i.e.  $pa \sim 90^\circ$ ). Weak east–west extensions on the 0.1-arcsec scale can also be seen on the map. The total flux density in an area  $0.2 \times 0.15$  arcsec of the map is  $4.25 \pm 0.1$  Jy, whereas model-fitting to the long baselines only gives a total flux density  $3.9 \pm 0.1$  Jy; thus the extended ( $\sim 0.1$  arcsec) structure around the nucleus has a flux density of  $0.35 \pm 0.15$  Jy. The comparison of the observed fringe-amplitudes and the transform of the delta functions which comprise the map of the whole  $2.2 \times 2.2$  arcsec field are shown in Fig. 3. More detailed observations with higher resolution are required to investigate the complicated structure of this central core.

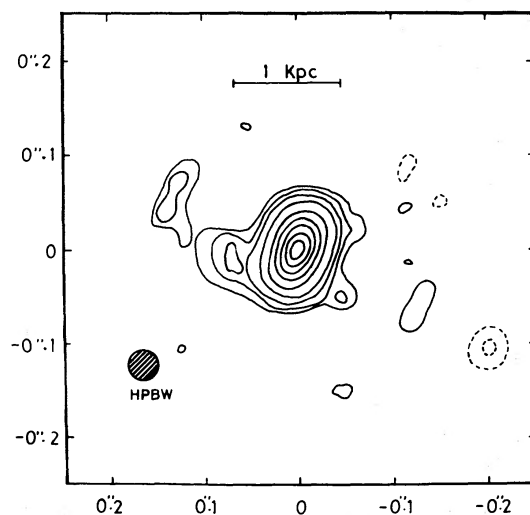


**Figure 2.** The hybrid map of the central component with a resolution of 30 milliarcsec. The contour intervals are:  $\pm 0.5, 1, 2, 5, 15, 30, 50, 70$  and 90 per cent of the peak value which corresponds to 2330 mJy per beam area. There is a  $180^\circ$  uncertainty in the orientation of this map.

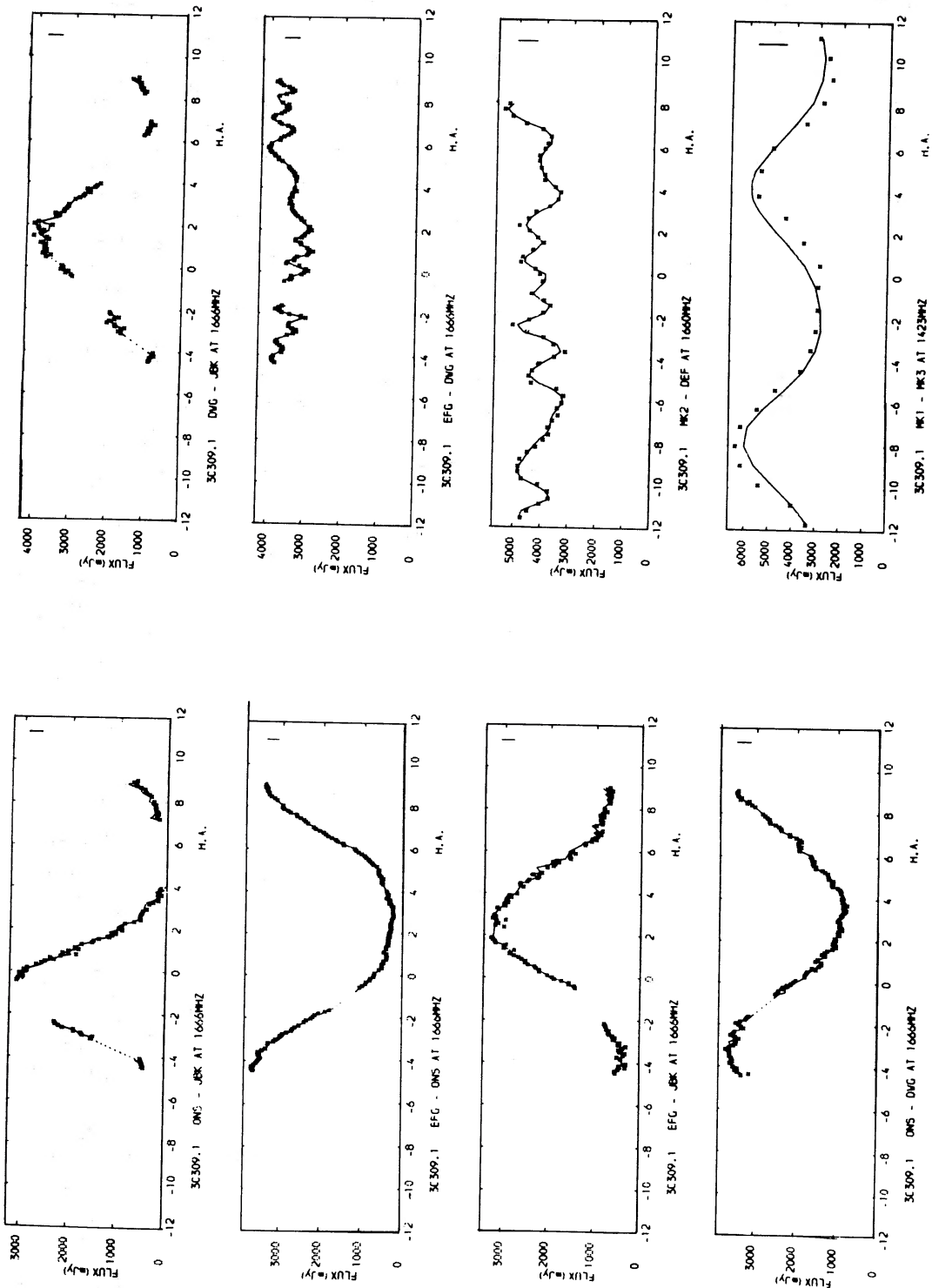


Figure 3. The fit to the fringe-amplitude data from delta functions comprising the  $2.2 \times 2.2$  arcsec map (see text). The amplitude uncertainties are indicated by the error bars in the top right-hand corner of each plot.

## 3.3 THE EXTENDED STRUCTURE

Hybrid maps were made starting from three different models and reasonably satisfactory fits to the fringe-amplitude data were achieved in each case; these maps are shown in Fig. 4 (a,b,c). Although the basic structure is similar in each case, there are detailed differences which illustrate the uncertainty resulting from the limited data available to us. The iterations resulting in Fig. 4 (a,b) were started from relatively complicated six- and five-component models respectively, whereas the map in Fig. 4(c) was started from only a two-component model. We have resolved the  $180^\circ$  position-angle ambiguity by comparing our brightness distributions with an unpublished VLA map (Wilkinson *et al.* in preparation) in which it is clear that the strongest outlying component is situated to the east of the nucleus. The major uncertainty in our maps is whether the weak component ( $\sim 120$  mJy) closest to the nucleus lies to the east or west. Because of our restricted data, we did not restore these maps with the conventional CLEAN beam, i.e. a Gaussian with the same FWHM as the main lobe of the dirty beam. In our case this was 0.1 arcsec, but we felt that a beam of 0.3 arcsec better represented our degree of confidence in the results. Formally the brightness distribution in Fig. 4(b) gives the best fit to the short-baseline data and this fit is virtually indistinguishable from that of the full map shown in Fig. 3. All the hybrid maps in Fig. 4 contain 94 per cent of the zero-baseline flux density and ascribe the same flux density to the central region (68 per cent); the ratio between the flux densities of the east and west components is  $1.9 \pm$

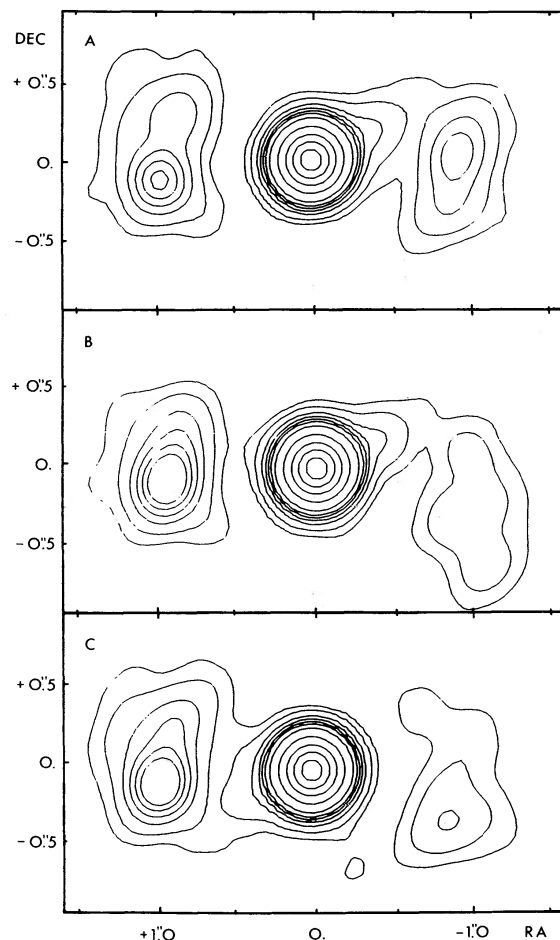


Figure 4. Hybrid maps of the extended structure made from three different initial models (for explanation see text). The contour intervals are: 1, 2, 4, 6, 8, 10, 15, 30, 50, 70 and 90 per cent of the peak value which corresponds to 4500 mJy per beam area.

0.4. The missing 6 per cent of the flux density could be accounted for by an extended ( $\geq 5$  arcsec) halo, but may be due merely to calibration uncertainties.

The overall source structure extends 2.6 arcsec east–west and 1.3 arcsec north–south. The outer components are highly resolved on baselines longer than  $\sim 3M\lambda$  and therefore do not contain structure smaller than  $\sim 50$  milliarcsec. There is an 0.40-Jy bright spot in the east component which lies  $1.03 \pm 0.03$  arcsec in pa  $95^\circ.5 \pm 0^\circ.5$  from the nucleus and has a diameter of  $\sim 100$  milliarcsec (0.85 kpc).

#### 4 The spectrum

In Fig. 5 we show a decomposition of the integrated spectrum into spectra of the nucleus and of the remaining extended structure. In addition to the present data, we have used VLBI data at 408 and 448 MHz (Brotten *et al.* 1969), 609 MHz (Wilkinson *et al.*, unpublished), together with VLA data at 5 GHz (Wilkinson *et al.*, in preparation) and Cambridge 5-km telescope data at 15 GHz (Laing 1981). The extended structure has a steep straight spectrum over the whole range from 100 MHz to 15 GHz, with a spectral index  $-0.94 \pm 0.08$ . This must peak at  $25 \pm 10$  MHz, giving an equipartition size (Scott & Readhead 1977) of  $1.2 \pm 0.5$  arcsec which is consistent with the size of the emitting regions on our hybrid maps. The nuclear spectrum is convex, showing clear signs of synchrotron self-absorption, but there is some uncertainty about the 5-GHz and 15-GHz values which were taken from lower resolution maps and could contain a contribution from a weak halo around the true nucleus. We have not located the spectral peak directly but it must occur around  $550 \pm 100$  MHz. This would imply an equipartition size of  $20 \pm 4$  milliarcsec which is not very different from the geometric mean (15 milliarcsec) of the major and minor axes estimated for the core.

#### 5 Discussion

Although our maps were made without phase data, we are confident that their major features are correct. On the scale of seconds of arc the source is clearly a triple with a compact, self-

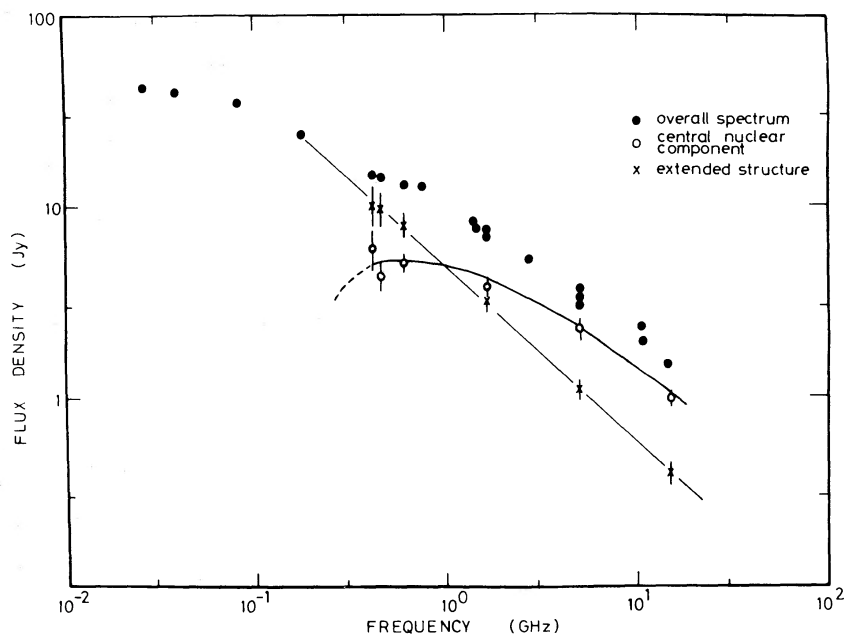


Figure 5. The spectrum of 3C 309.1 showing the contributions from the compact and extended components.

absorbed, central component and two steep-spectrum outer components ( $\alpha = -0.94$ ) whose flux ratio is about 2:1. For  $H_0 = 50 \text{ km s}^{-1} \text{ Mpc}^{-1}$  and  $q_0 = \frac{1}{2}$ , the overall projected linear size is  $22 \times 11 \text{ kpc}$ . Perhaps the most striking feature in 3C 309.1 is the dramatic change in position angle between the core and the outer structure. This change in position angle, measured with respect to the hot spot in the east component, is  $66^\circ$  but is even larger ( $80^\circ$ ) with respect to a line joining the centroids of the outer components. The rotation in position angle apparently occurs within  $\sim 0.1 \text{ arcsec}$  ( $\sim 1 \text{ kpc}$ ) of the nucleus. Until now, such behaviour was thought to occur only in the one-sided (D2) quasars (Readhead *et al.* 1978; Davis *et al.* 1978; Readhead 1980), and this is the first time that a source with extended structure on both sides of the core has been shown to exhibit such a large rotation in position angle.

The dominance of the central core above 1 GHz, and the small overall size, means that 3C 309.1 is a type-C source as defined by Readhead *et al.* (1978). Until very recently, those few type-C sources whose extended structure had been investigated in any detail were found to be one-sided, and thus this classification was thought to be identical to the D2 class defined by Miley (1971). New measurements with the VLA (Perley, Fomalont & Johnston 1980) have shown, however, that the presence of weak extended structure near compact radio sources is not only common but also not exclusively one-sided. Thus the two classifications are *not* identical. Perley *et al.* conclude that at least the two-sided sources might be normal doubles, with exceptionally bright central cores, viewed nearly end-on.

Can this hypothesis be reconciled with our observations of 3C 309.1? Certainly the large apparent change in position angle is consistent with the idea that we are viewing a curved jet close to the line-of-sight. This intrinsic curvature need only be slight ( $\sim 5^\circ$ ) and may be in a single plane but, depending on the exact angle to the line-of-sight, one can account for the magnification of the bending angle by an order of magnitude and for the fact that it apparently occurs close to the origin. This model has been suggested for other type-C sources and particularly those exhibiting superluminal velocities (Readhead *et al.* 1978). Thus the core could be intrinsically weak but enhanced by relativistic beaming (Scheuer & Readhead 1979; Blandford & Königl 1979). Although it is not possible to test this idea quantitatively because there are too many free parameters to be assigned, the following plausibility argument shows that our observations can be interpreted in this way. Let us assume  $\gamma = 2$  (the value suggested by Scheuer & Readhead for normal doubles),  $\theta = 5^\circ$ , where  $\theta$  is the angle between the beam and the line-of-sight, and note that at 5 GHz the flux ratio between the core and outer lobes is  $\sim 2$ . Then applying Scheuer & Readhead's equation (1), we find that the core flux density is amplified by  $\sim 400$  compared with the outer lobes which are assumed to radiate isotropically. Thus these assumptions would imply that the intrinsic flux ratio between core and outer lobes is  $5 \times 10^{-3}$  and the total extent of the source is  $\sim 250 \text{ kpc}$ . These are consistent with observations of other quasars which show normal double structure (Jenkins, Pooley & Riley 1977; Gopal-Krishna 1980).

Alternatively, of course, the major axis could lie in the plane of the sky. In this case 3C 309.1 would really be a new type of source, i.e. a compact triple with an intrinsically powerful nucleus which must have rotated relative to the outer lobes by  $\sim 80^\circ$ . One way to differentiate between these two possibilities is to look for superluminal motions in the core. These would be *prima facie* evidence that the source axis is close to the line-of-sight, for this special geometry is required by most current theories of the superluminal phenomenon. In fact 3C 309.1 provides a good opportunity for testing these theories on other than D2 sources, for its nucleus is quite strong at 5 and 10 GHz so the necessary high-resolution VLBI observations are feasible.

To summarize then, 3C 309.1 shows characteristics of both D2 and D1 quasars and could well be a normal double source viewed almost along its major axis. A more stringent test of

this hypothesis requires more detailed observations with a higher dynamic range, both of the central core and the extended structure. Such observations are being made or are planned with the Jodrell Bank Multi-Telescope-Radio-Linked-Interferometer (MTRLI) and with the European VLBI Network.

### Acknowledgments

We thank the directors and staff of all the observatories involved in this work and in particular B. Rönnäng and L. Baath at Onsala, R. T. Schilizzi and A. van Ardenne at Dwingeloo, and J. R. Baker, I. Pauliny-Toth and K. Weiler at MPIfR, Bonn for their help in the observations. We are also indebted to D. Graham and H. Blaschke for help in processing the data. These were among the first observations to be processed using the MPIfR processor and we are grateful to everyone in Bonn who contributed to their success.

PNW acknowledges the receipt of a Royal Society Weir Fellowship, and AJK gratefully acknowledges his debt to Manchester University and the British Council for his research fellowship and in particular to Professor Sir Bernard Lovell for his encouragement and support.

### References

- Baldwin, J. E. & Warner, P. J., 1978. *Mon. Not. R. astr. Soc.*, **182**, 411.  
 Blandford, R. D. & Königl, A., 1979. *Astrophys. J.*, **232**, 34.  
 Broten, N. W., Clarke, R. W., Legg, T. H., Locke, J. L., Galt, J. A., Yen, J. L. & Chisholm, R. M., 1969. *Mon. Not. R. astr. Soc.*, **146**, 313.  
 Burbidge, G. R. & Burbidge, E. M., 1969. *Nature*, **222**, 735.  
 Clark, B. G., Kellermann, K. I., Bare, C. C., Cohen, M. H. & Jauncey, D. L., 1968. *Astrophys. J.*, **153**, 705.  
 Clark, B. G., 1973. *Proc. IEEE*, **61**, 1242.  
 Davis, R. J., Stannard, D. & Conway, R. G., 1978. *Mon. Not. R. astr. Soc.*, **185**, 435.  
 Fort, D. N., 1971. *PhD Thesis*, Manchester University.  
 Fort, D. N. & Yee, H. K. C., 1976. *Astr. Astrophys.*, **50**, 19.  
 Gopal-Krishna, 1980. *Astr. Astrophys.*, **86**, L1.  
 Högbom, J. A., 1974. *Astr. Astrophys. Suppl.*, **15**, 417.  
 Jenkins, C. J., Pooley, G. G. & Riley, J. M., 1977. *Mem. R. astr. Soc.*, **84**, 61.  
 Kellermann, K. I., Jauncey, D. L., Cohen, M. H., Shaffer, D. N., Clark, B. G., Broderick, J., Rönnäng, B., Rydbeck, O. E. H., Matveyenko, L., Moiseyev, I., Vitkevitch, V. V., Cooper, B. F. C. & Batchelor, R., 1971. *Astrophys. J.*, **169**, 1.  
 Laing, R. A., 1981. *Mon. Not. R. astr. Soc.*, **194**, 301.  
 Miley, G. K., 1971. *Mon. Not. R. astr. Soc.*, **152**, 477.  
 Perley, R. A., Fomalont, E. B. & Johnston, K. J., 1980. *Astr. J.*, **85**, 649.  
 Readhead, A. C. S., 1980. *IAU Symp. No. 92*, in press.  
 Readhead, A. C. S., Cohen, M. H., Pearson, T. J. & Wilkinson, P. N., 1978. *Nature*, **276**, 768.  
 Readhead, A. C. S. & Wilkinson, P. N., 1978. *Astrophys. J.*, **223**, 25.  
 Ryle, M. & Elsmore, B., 1973. *Mon. Not. R. astr. Soc.*, **164**, 223.  
 Scheuer, P. A. G. & Readhead, A. C. S., 1979. *Nature*, **277**, 182.  
 Scott, M. A. & Readhead, A. C. S., 1977. *Mon. Not. R. astr. Soc.*, **180**, 539.  
 Wilkinson, P. N., 1972. *Mon. Not. R. astr. Soc.*, **160**, 305.  
 Wilkinson, P. N., 1973. *Jodrell Bank Annals*, **2**, 58.  
 Wilkinson, P. N., Readhead, A. C. S., Purcell, G. H. & Anderson, B., 1977. *Nature*, **269**, 764.